

Battery cell configuration for organic light emitting diode display in modern smartphones and tablet-PCs *

Donghwa Shin, Kitae Kim[†]
and Naehyuck Chang[†]
Department of Electrical Engineering and
Computer Science
Seoul National University
{dhshin, ktkim, naehyuck} @elpl.snu.ac.kr

Massoud Pedram
Department of Electrical Engineering
University of Southern California
pedram@usc.edu

ABSTRACT

Modern smartphones and tablet-PCs are equipped high-resolution and large-size display, which is a primary power consumer. Despite of power efficiency of organic light emitting diode (OLED) display nature, the integrated display subsystem exhibits low energy efficiency due to power loss in the battery and voltage boost conversion. In this paper, we discover energy efficiency in terms of the battery internal loss as well the converter circuit efficiency by the OLED power supply condition. We also analyze the effect of recently introduced OLED dynamic (driver) supply voltage scaling technique on the system-level efficiency while considering the real aspect of the system-level power consumption. We introduce the optimal battery setup for different size and resolution of OLED display for modern smartphones and tablet-PCs.

1. INTRODUCTION

Modern mobile devices such a smartphone or tablet PC are typically equipped with a multi-core gigahertz processor, gigabytes of high-speed DDR SDRAM, dozens of gigabytes of flash memory, several up to 10 megapixel cameras, 1M+ pixel high-resolution color display, high-power audio, as well as 3G/4G, Wi-Fi and Bluetooth wireless communication devices. As a result, modern mobile devices suffer from the short battery lifetime. As reported in [1], average power conversion efficiency in the smartphone is merely around 60% to 70%. Although there has been numerous effort on the development of low-power techniques from transistor-level to system-level, if we cannot enhance the power conversion efficiency, even cutting-edge low-power techniques cannot meaningfully increase the battery lifetime. Therefore, power conversion

*This work is sponsored by a grant from the National Science Foundation, the Brain Korea 21 Project, and the National Research Foundation of Korea (NRF) grant funded by the Korean Government (MEST) (No. 2011-0016480 and 2011-0030512). The ICT at Seoul National University provides research facilities for this study.

[†]Corresponding author

Permission to make digital or hard copies of all or part of this work for personal or classroom use is granted without fee provided that copies are not made or distributed for profit or commercial advantage and that copies bear this notice and the full citation on the first page. To copy otherwise, to republish, to post on servers or to redistribute to lists, requires prior specific permission and/or a fee.

Copyright 2012 ACM ...\$10.00.

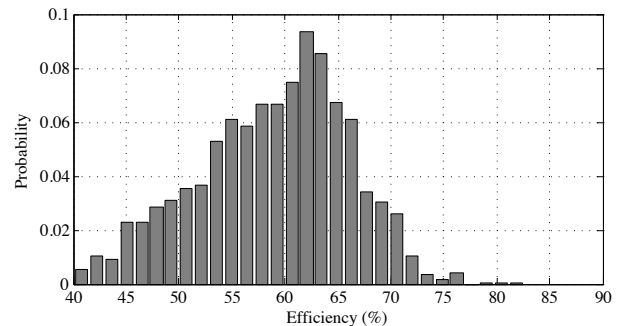


Figure 1: Average power efficiency histogram of Snapdragon MDP for the benchmark applications.

efficiency should be considered to extend the battery lifetime.

We measure the power consumption of the smartphone platform by using Snapdragon MDP from Qualcomm [2]. For the experiment, we develop a benchmark which is designed to sequentially enable the system components in the platform and change the operating status. Figure 1 shows the result of efficiency profiling. System level power efficiency is about 60%. It is quite low value beyond common expectation while the efficiency of the commercial DC-DC converters are known to be higher than 90%. The switching-mode DC-DC converters show high efficiency only when they are appropriately integrated to the system.

It is well known that the efficiency of the power converters is dependent on its input/output voltage and current. A switching converter consumes part of input power to switch the MOSFET switches. Power dissipation by parasitic resistance in the MOSFET switches and passive devices such as an inductor and a capacitor also cannot be ignored. Those power losses are dependent on the input/output voltage and current. Furthermore, power loss in a linear regulator is directly proportional to the voltage difference and current through the regulator.

The major power consumers in the modern mobile systems are an application processor (AP), wireless interfaces, and display. Modern AP and wireless interface ICs accept lower than the output voltage of 1-cell Li-ion battery. Therefore, from the perspective of the power conversion efficiency, it is better to supply the input voltage to the converter as low as possible. However, unfortunately, the display devices generally require much higher voltage than the silicon devices in the system. LCDs and OLED displays commonly accept 12 V or higher voltage to illuminate

themselves. Their input voltage is determined by the electrical and optical characteristics of the display cell elements and light source. Several OLED display panel modules accept 3.7 V (1-cell Li-ion battery) as an input [3], but it internally boosts the input voltage by using the charge pumps to generate the input voltage to the OLED cells. As a result, the battery setup should be determined while considering both step-down conversion and step-up conversion. To derive the optimal setup, We need to consider the power conversion efficiency of the system components and behavioral characteristics of the components.

However, the smartphones and tablet PCs are designed only by a legacy design rule so far. Smartphones and tablet PCs from major vendors such as Apple or Samsung uses 1 cell Li-ion battery while the laptop PC typically have 3 cells or more Li-ion batteries. Especially, modern tablet PCs which equip a several GHz multi-core processor and up to 10" size high-resolution display still use 1 cell Li-ion battery because of the legacy design rule and compatibility issues though its hardware is close to Laptop PC rather than smartphone. It is time to examine the effectiveness of the legacy design rule.

In this paper, we introduce a systematic approach to design the power conversion architecture considering the behavioral characteristics of the system. We introduce an estimation model power conversion efficiency based on the system activity analysis. Based on the model, we maximize the power conversion efficiency by changing the battery setup. We also consider the internal characteristics of the batteries to optimize the battery setup and the effect of recently introduced OLED dynamic (driver) supply voltage scaling technique (OLED DVS) [4] on the system-level power efficiency.

The rest of the paper is organized as follows. Section 2 introduces previous research on the system-level low-power techniques for the display system. Section 3 explains the the characteristics of the OLED cell and driver circuits and introduces the principles of the supply voltage scaling. Section 4 presents power converter efficiency models and system-level estimation method. Section 5 introduces the battery model and explains the battery setup optimization process. Finally, Section 6 concludes the paper.

2. RELATED WORK

There are numerous studies on power analysis and modeling of the computing systems including not only and general-purpose systems but also mobile embedded systems. The majority of existing studies focus on specific components in the system. We can find a lot of power models for each device such as microprocessors, memory devices, wireless communications, those models are usually too complicated for application development. The power management of microprocessor is well studied in [5]. A low-power techniques for OLED display considering the efficiency of driver circuits is introduced in [4].

Several system-level activity profiling-based power model for the mobile computing system has been introduced. A Measurement based power estimation model was introduced in [6, 7, 8]. They collect the system activity parameter and measure the system power consumption. The power coefficients are derived by regression analysis. A simulation technique based on an energy-state model and cycle-accurate characterization was introduced in [9]. A performance monitoring unit was designed by using a variable reduction technique. Recently, battery-behavior monitoring-based approaches have been introduced. An adaptive modeling method based on the battery monitoring was introduced in [10]. Some method used a embedded voltage, current, and temperature sensor for batteries to automatically build the system-level power model [11]. They usually model the system with an analytical

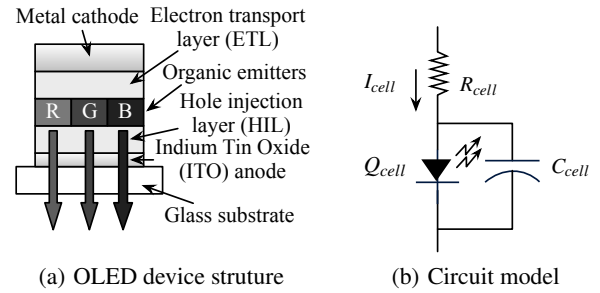


Figure 2: Device structure of OLED and equivalent circuit model.

equations, and provide automatic coefficient deriving method. Based on the power consumption characteristics of the system, DC-DC converter reconfiguration technique is introduced to enhance the power efficiency [12].

Battery models for the electronic systems have extensively been studied during the past few decades. We can find many analytical models based on electrochemical modeling and analysis [13, 14], but the electrochemical battery models are too complicated to be used for the system-level design of electronics. Battery models in the form of an electric circuit are suitable for this purpose [15, 16].

3. DYNAMIC (DRIVER) SUPPLY VOLTAGE SCALING OF OLED DISPLAYS

3.1 OLED cell architecture

Figure 2(a) shows the typical structure of the OLED cell [17]. The OLED device has a large area, but the thickness of the organic layers between the electrodes is only 100–200 nm. As a result, OLED cells have a large internal capacitance. The internal capacitance is not constant, but depends on the voltage and switching frequency. The value of C_{cell} is typically 200–400 pF/mm². OLED cells have a resistive component for each layer that lies between anode and cathode. The dominant resistive component is caused by the transparent Indium-Tin-Oxide (ITO) layer. Hence, the parasitic resistor is in series with the internal capacitance. The value of the parasitic resistor is strongly dependent on the design of the ITO electrode (anode). A typical value of the cell resistance is 15Ω/sq¹. We calculate the R_{cell} with the cell area and sheet resistance. A simple equivalent circuit obtained with the physical parameters is depicted in Figure 2(b). It consist of the parasitic resistor R_{cell} , internal capacitance C_{cell} , and a diode Q_{cell} .

The structure and materials used to implement the OLED cell make the cell requires higher voltage to drive it. The organic emitter materials requires 3-5 V to illuminate itself, and the parasitic resistance becomes large due to its thin shape for the transparency. Therefore, the OLED cell requires relatively higher supply voltage compared to the other silicon devices in the system and the 1-cell Li-ion battery which is generally used for the smartphone-like mobile systems.

3.2 OLED display panel structures and driver circuits

The OLED cell current, I_{cell} , determines its luminance. The cell current is basically controllable by adjusting the cell voltage, V_{cell} . However, because the parasitic resistance is not stable, we

¹Ω/sq denotes the sheet resistance.

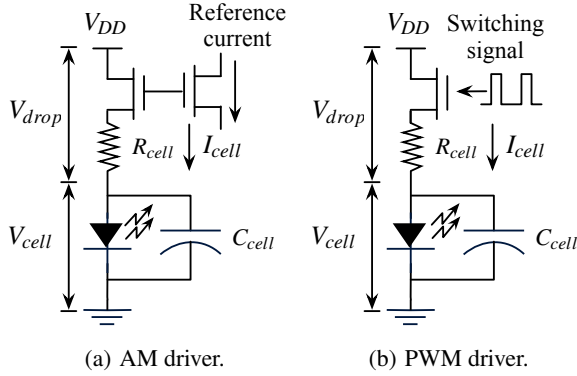


Figure 3: Behavioral concept of AM driver and PWM driver for the OLED display.

commonly use a constant current driver. We can easily make a constant current source with a current mirror. We call an OLED driver using a current mirror-based current steering circuit an amplitude modulation (AM) driver. AMOLED panels are typically controlled by an AM driver circuit. There is a current source transistor whose gate voltage is maintained by a storage capacitor in the AM AMOLED driver. The AM driver scheme ensures a higher reliability and efficiency of the OLED cells. However, the current steering circuit consumes large area, which results in higher cost.

On the other hand, PMOLED panels have a row-column structure driver circuit. There is no storage capacitor in the PMOLED driver circuit. The cell current can be a pulsed current. We can easily achieve a pulse width modulation (PWM) of the cell current in the PMOLED panels. The luminance of an OLED cell is actually dependent on the average value of I_{cell} . The PWM cell current steering is inexpensive and provides precise luminance control. However, it is known to be less power efficient in high luminance region [17]. Unfortunately, the PWM driver in AMOLED panels is expensive. Some AMOLED drivers use both PWM and AM at the expense of even higher cost to tackle both display quality and power consumption.

3.3 Effect of V_{DD} scaling on driver circuits

The concept of DVS of an OLED panel is to reduce power loss due to V_{drop} by scaling down V_{DD} . Although we scale down the V_{DD} of the AM driver circuit, there is only small change in I_{cell} due to the Early Effect in the AM driver as far as the driving transistor remains in the saturation mode (Figure 3 (a)). The driving transistor is in the triode mode when I_{cell} becomes too large with the scaled V_{DD} . The cell luminance decreases as we scale down V_{DD} in the triode mode, which causes image distortion.

The power loss of OLED cell is defined by $P_{loss} = I_{cell}V_{drop}$ where V_{drop} is determined by the characteristics of the OLED cell and I_{cell} is determined by the saturation current of the driver transistor. The excessive power should be dissipated by the driver transistor, and P_{loss} is given by

$$P_{loss} = I_{cell}V_{drop} = I_{cell}(V_{DD}V_f), \quad (1)$$

where V_f is the forward bias voltage of the diode.

DVS acts a bit differently in a PWM driver (Figure 3 (b)). Scaling V_{DD} down directly affects I_{cell} . We have to restore the luminance of image even with a slight V_{DD} scale. We apply a model-based image compensation and restore the luminance. A brighter color makes a higher PWM duty ratio in the PWM driver. The image compensation cannot always restore the original luminance if the original I_{cell} is too large. The maximum possible I_{cell} under

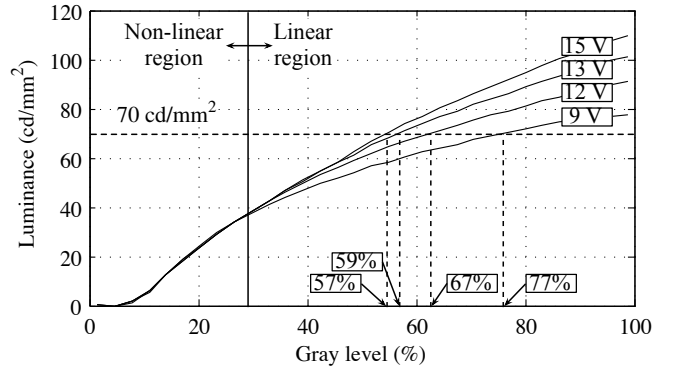


Figure 4: Measured luminance by V_{DD} and gray level with AM driver.

the scaled V_{DD} cannot be the same as the original I_{cell} even when the PWM duty ratio is set to 100%. Thus, luminance distortion for some very bright pixels becomes unavoidable. We sacrifice a small display quality by allowing a certain amount of color distortion of the image but save significant amount of power consumption.

With the PWM drivers, V_f and R_{cell} determine the maximum value of I_{cell} as follows:

$$I_{cell} = \frac{V_{DD}V_f}{R_{cell}}. \quad (2)$$

The luminance of the OLED is approximately proportional to the average value of I_{cell} , $\overline{I_{cell}}$, which is calculated by

$$\overline{I_{cell}} = I_{cell}d = I_{cell} \frac{t_{on}}{t_{on} + t_{off}}, \quad (3)$$

where PWM duty, $d = t_{on}/(t_{on} + t_{off})$, and t_{on} and t_{off} are the switch turn on and off durations in a PWM period, respectively. The power loss of an OLED cell during a PWM period is given by

$$P_{loss} = \overline{I_{cell}}^2 R_{cell}. \quad (4)$$

We visualize a part of characterization data in Fig. 4. The OLED display achieves the same luminance by adjusting the color value (gray level here), corresponding to the PWM duty, even with different V_{DD} levels. In other words, we can restore the color value with even a reduced V_{DD} , which proves the key premise of DVS for OLEDs. Fig. 4 shows that the OLED panel generates a 70 cd/mm² luminance with a 15 V, a 13 V, a 11 V, and a 9 V V_{DD} by setting the gray level to 57%, 59%, 64%, and 77%, respectively. It turns out that the luminance is not affected by V_{DD} when the gray level is below a certain level such as non-linear region in Fig. 4. Therefore, we compensate the V_{DD} scaling-induced luminance reduction by modifying image data only in the linear region of Fig. 4.

4. POWER EFFICIENCY ANALYSIS

4.1 Power converter efficiency

4.1.1 Switching-mode DC-DC converter power loss model

The power loss model of a DC-DC converter is well-studied in [12]. In general, the major sources of power loss in a DC-DC converter are conduction loss, switching loss in the power switches, and controller power loss. We denote them as $P_{conduction}$, $P_{switching}$, and $P_{controller}$, respectively. The switching-mode DC-DC converters can be implemented by using a switch and a diode

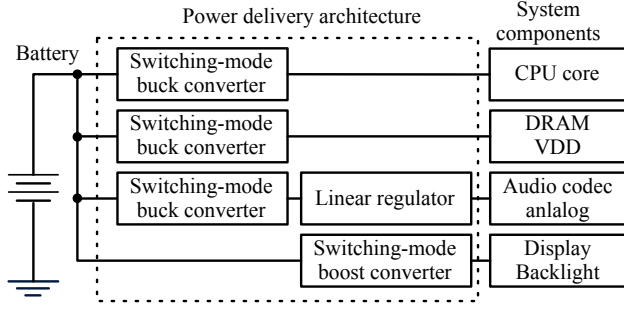


Figure 5: Power conversion architecture concept.

or two switches. The switching-mode DC-DC converters using two switches basically replace the diode with the synchronous switch (lossless diode) to avoid the power loss due to the voltage drop in the diode. It shows better efficiency but also requires more components and complicated control. Power loss in the switching mode DC-DC converter with the synchronous switch in continuous mode is approximately given by

$$P_{loss}^{sw} = P_{conduction} + P_{switching} + P_{controller} \quad (5)$$

$$P_{conduction} = I_{out}^2(R_L + DR_{sw1} + (1-D)R_{sw2}) + \frac{1}{3}\left(\frac{\Delta I}{2}\right)^2(R_L + DR_{sw1} + (1-D)R_{sw2} + R_C)$$

$$P_{switching} = V_{on}f_s(Q_{sw1} + Q_{sw2}),$$

where f_s is the switching frequency; and $I_{controller}$ denotes the current used in the control logic section of the converter. Series resistances of the inductor L and capacitor C are denoted by R_L and R_C , respectively. Similarly, series resistances of the two MOSFET switches are represented by R_{sw1} and R_{sw2} , respectively, while the amounts of their gate charge are denoted by Q_{sw1} and Q_{sw2} , respectively. V_{on} denotes turn on input voltage of the MOSFET gate and Q_{sw} is equals to $C_{sw} * V_{on}$. ΔI represent the inductor current ripple. ΔI for the buck converter, ΔI_{buck} , and boost converter, ΔI_{boost} , with the input voltage, V_{in} , and output voltage, V_{out} , are given by

$$\Delta I_{buck} = \frac{V_{in} - V_{out}}{L} \frac{V_{out}}{f_s}, \quad (6)$$

$$\Delta I_{boost} = \frac{V_{in}}{L} \left(1 - \frac{V_{in}}{V_{out}}\right).$$

If we use the diode, $P_{conduction}$ should be changed to as follows:

$$P_{conduction} = I_{out}^2(R_L + DR_{sw1} + (1-D)R_{sw2}) + \frac{1}{3}\left(\frac{\Delta I}{2}\right)^2(R_L + DR_{sw1} + (1-D)R_{sw2} + R_C), \quad (7)$$

4.1.2 Linear regulator power loss model

A typical linear regulator consists of an error amplifier, a pass transistor, and a feedback resistor network. The power loss of the linear regulator, denoted by P_{linear} , is given by:

$$P_{loss}^{linear} = I_{out}(V_{in} - V_{out}) + I_q V_{in}, \quad (8)$$

I_q denotes the quiescent current of the linear regulator. The power loss of the linear regulator is proportional to the difference between input and output voltage. The pass transistor solely dissipates the power difference between input and output.

4.2 Equivalent efficiency model of power conversion path

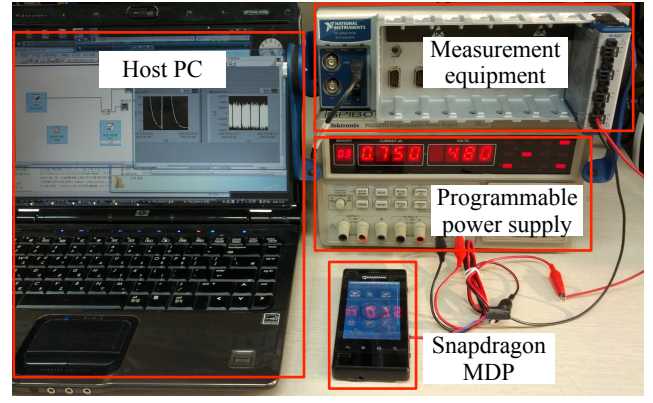


Figure 6: Experimental setup for power characterization of Snapdragon MDP development platform.

In typical mobile devices, the power conversion loss in the path can be regarded as a combination of P_{loss}^{sw} and P_{loss}^{ldo} . The switching converters are generally used to generate a specific voltage for the components due to the conversion efficiency and heat dissipation. The linear regulators are typically placed between the switching converter and components which require low-noise voltage supply as illustrated in Figure 5. The linear regulators are only used for the step-down conversion.

For step-down conversion, we model the equivalent power loss for the path in terms of the combination of P_{loss}^{sw} and P_{loss}^{ldo} from (5), (6), (7), and (8). P_{loss} model for step-down conversion with a fixed output voltage is given by

$$P_{loss}^{conv} = a_1 I_{out}^2 + a_2 I_{out} + \frac{a_3}{V_{in}^2} + \frac{a_4}{V_{in}} + a_5 V_{in} + a_6 \quad (9)$$

where V_{in} and I_{out} denote a system input voltage from the battery and output current to the components and a_1 to a_6 represent the coefficient which are obtained by the regression of the measured P_{loss} .

For the system with multiple subcomponents, the system-level P_{loss}^{sys} can be calculated by summing the component-level $P_{loss}^{conv,i}$, which is given by

$$P_{loss}^{sys} = \sum P_{loss}^{conv,i} \quad (10)$$

$$= \sum (a_1^i I_{out}^2 + a_2^i I_{out} + \frac{a_3^i}{V_{in}^2} + \frac{a_4^i}{V_{in}} + a_5^i V_{in}) + a_6$$

where n denotes the number of subcomponents in the system.

4.3 Power conversion efficiency analysis of smartphone platform

We use the MSM8660 SnapDragon MDP from Qualcomm as a target platform [2]. The SnapDragon MDP incorporates embedded power sensors that monitors fine-grain module (a set of devices) current values. It is a cutting-edge development platform for the smartphone equipped with Google Android OS 2.3 on the top of Snapdragon 1.5 GHz asynchronous dual-core CPU, a 3D-supporting GPU, 3.61" WVGA multi-touch screen, 1 GB internal RAM, 16 GB on-board flash, Wi-Fi, Bluetooth, a GPS, dual-side cameras, etc. However, since its primary purpose is to develop prototype applications, it does not have a cellular module. We perform power measurement of each modules using the application profiling tool named *Treppn*TM.

Table 1: Target platform components

Component	Supply Voltage (V)	Average current (mA)	Current standard deviation
Audio DSP	1.1	0.5195	0.6332
VREG L16A	1.8	5.7261	6.8969
SD Card	2.85	0.3182	1.434
Audio Codec IO	1.8	0.0543	0.0603
Audio Codec VDDCX 1	1.2	0.0552	0.0604
Audio Codec Analog	2.2	0.0858	0.092
Touch Screen	2.85	3.4592	3.7758
CPU Core 0	0.9-1.2	29.6233	48.8773
Internal Memory	1.1	11.9731	13.1627
CPU Core 1	0.9-1.2	29.5807	50.1398
eMMC	2.85	0.0901	0.5602
Digital Core	1.1	71.6834	75.1188
ISM VDD2	1.35	0.1208	0.1326
IO PAD3	1.8	1.9533	2.4165
IO PAD2	2.85	0.0948	0.2627
Haptics	2.6	3.8972	3.9384
VDDPX1 LPDDR2	1.2	4.3597	5.4995
DRAM VDD1	1.8	0.4462	0.505
Ambient Light Sensor	2.85	0.0716	0.0748
Display ELVDD	3.8	5.2717	13.091
Display IO	1.8	0.0603	0.0815
Display Memory	3	2.8102	3.7988
eMMC Host Interface	1.8	0.0549	0.3631
HDMI	5	0.0388	0.0555
Camera IO	1.8	0.1084	0.1374
Camera Digital	1.2	0.051	0.0669
Camera Analog	2.85	0.0494	0.071
DRAM VDD2	1.2	4.23	5.9156

We develop a benchmark application to enable component-wise activity control. The benchmark generates various usage patterns by repeatedly activating each component with minimum to maximum utilization while other components are disabled to reduce the correlated power consumption. We utilize some component sets simultaneously to simulate real usage patterns. We randomly change the activated time to avoid the same periodic patterns. The benchmark controls following components:

CPU The benchmark generates cache hits and misses through matrix traversal operations. After create a 2048×2048 integer matrix in the main memory, in order to calculate simple summation, load the integers sequentially from the matrix in row-major order and column-major order alternately. After these repetition, Fast Fourier transform (FFT) is executed for full utilization.

GPU GPU is utilized through matrix manipulations such as cropping, rotating, skewing, resizing, and rendering bitmap images.

DSP We play high-quality video and audio files encoded various codecs.

Wi-Fi We downloads files which have different size from a web server via Hypertext Transfer Protocol (HTTP).

Display We changes the screen brightness from 0% to 100%

Table 2: Extracted parameters for power loss model

Component	a_1	a_2	a_3	a_4	a_5	a_6
CPU Core0	2.045e-4	7.152e-1	5.444e-4	1.217e-4	2.490e-3	7.641e-6
CPU Core1	3.003e-4	5.703e-1	5.312e-4	2.236e-5	2.641e-3	
Digital core	3.093e-3	7.133e-1	5.353e-4	2.026e-5	2.599e-3	
Internal memory	1.081e-3	8.456e-1	5.353e-4	2.027e-5	2.597e-3	
VREG L16A	9.451e-4	8.235e-1	5.209e-4	5.672e-5	2.609e-3	
VDDPX1 LPDDR2	8.788e-4	5.967e-1	5.329e-4	2.470e-5	2.502e-3	
DRAM VDD2	7.638e-4	6.286e-1	5.330e-4	2.471e-5	2.601e-3	
Display ELVDD	8.401e-3	1.571e0	2.340e-14	5.244e-4	5.011e-3	

GPS A GPS module is activated to locate current position of the smartphone during random periods.

We characterize the power consumption of the components in the target platform with the benchmark. The target platform provides 29 measurement point with embedded current sensor. We measure the current by using *Treppn*TM profiler with 100 ms sampling period. The supply voltage and current statistics is summarized in Tables 1. We select the components whose standard deviation of the current is greater than 5 to obtain meaningful regression result with sufficient I_{out} values. We connect the PG2521 programmable power supply from Tektronix to the battery connector of the target platform to maintain the V_{in} during the measurement. The measurement environment is presented in Figure 6. We change the V_{in} by adjusting the output voltage of the programmable power supply. The estimation model is obtained by regression analysis with Levenberg-Marquard curve-fitting method. The extracted parameters are summarized in Table 2. The P_{loss} model shows less than 1% average estimation error. The estimation result is presented in Figure 7.

5. BATTERY SETUP OPTIMIZATION

Figure 8 show the relation between the voltage setup of the

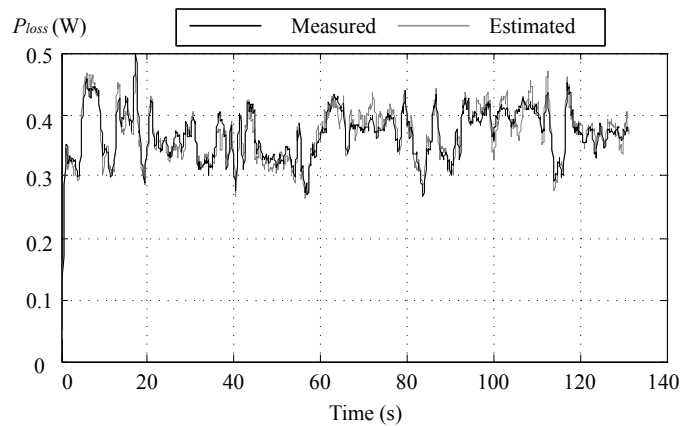


Figure 7: P_{loss} measurement result from the target platform and P_{loss} estimation result by the regressed model.

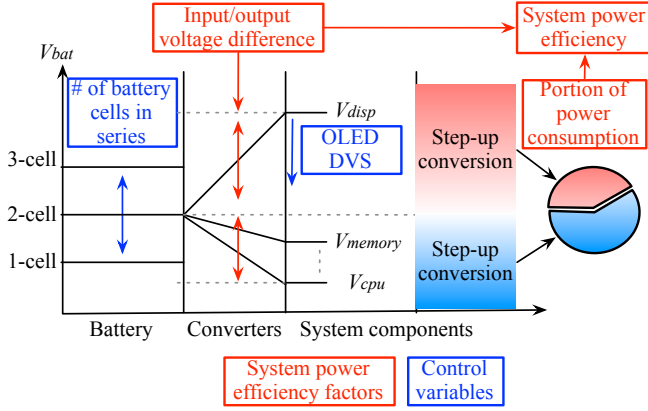


Figure 8: System-level power efficiency with battery setup and OLED DVS.

system and its power efficiency. The supplied voltage values to the ICs and display are determined by its behavioral characteristics and opto-electrical characteristics. The portion of power consumption and corresponding conversion efficiency finally determine the system power efficiency. The system should be optimized under the consideration of the voltage setup and corresponding conversion efficiency. We can increase the input voltage of the conversion circuits from the battery by changing the battery setup and decrease the output voltage of the setup-up converter to the display by using OLED DVS. The battery voltage can be set in discrete manner by changing the number of the cells in series. The OLED DVS reduces the supply voltage to the display on average. Consequently, we can extend the available design space when we use those two techniques at the same time.

5.1 Boost conversion efficiency model

Ordroid-A platform equips a MAX1790 switching-mode boost converter from Maxim [18]. We estimate the power efficiency of the boost converter by using the power loss model introduced in Section 4. We use the physical parameters of CDMC6D28NP-4R7MC power inductor from Sumida corporation [19], B120/B rectifier diode from Diodes inc. [20], and several capacitors from Taiyo Yuden [21]. The simulation parameters are summarized in Table 3.

The efficiency simulation result is illustrated in Figure 9. We change the input voltage from 3.7 V (1-cell Li-ion battery) to 11.1 V (3-cell Li-ion battery) output voltage. The output current is up to 1600 mA which is the maximum rating of MAX1790. It shows that the efficiency is very high with small output current due to the static power consumption of the boost converter including controller power and switching power. The efficiency gradually decreases after peak point because of the conduction loss. The input voltage affects the duty ratio of the PWM switch control and degrades the efficiency as the difference between the input and output voltage increasing.

Table 3: MAX1790 Boost converter simulation parameters.

Parameter	Value	Parameter	Value
L	4.7 μH	R_L	46.4 $\text{m}\Omega$
f_s	1.2 MHz	R_C	0.9 $\text{m}\Omega$
R_{sw1}	21 $\text{m}\Omega$	R_{sw2}	21 $\text{m}\Omega$
C_{sw1}	12.8 pF	C_{sw2}	12.8 pF
R_d	20 $\text{m}\Omega$	V_f	0.5 V

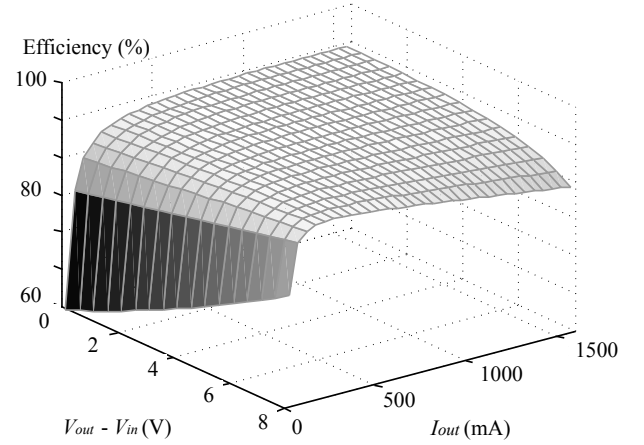


Figure 9: Simulation result of MAX1790 boost converter efficiency.

5.2 Battery model

Battery models for the electronic systems have extensively been studied during the past few decades. We have found many analytical models based on electrochemical process modeling and analysis [13, 14], but the electrochemical battery models are too complicated to be used for the system-level design of electronics. Rather, battery models in the form of an electric circuit are much more suitable for this purpose [15, 16].

We import a circuit model of the Li-ion battery from [16] as shown in Figure 10. This includes a runtime-based model as well as a circuit-based model for accurate capturing of the battery service life and I-V characteristic. We can describe the behavior of a Li-ion battery with the equivalent circuit and the following non-linear equations:

$$\begin{aligned}
 v_{OC} &= b_{11}e^{b_{12}v_{SOC}} + b_{13}v_{SOC}^3 + b_{14}v_{SOC}^2 + b_{15}v_{SOC} + b_{16}, \\
 R_s &= b_{21}e^{b_{22}v_{SOC}} + b_{23}, R_{ts} = b_{31}e^{b_{32}v_{SOC}} + b_{33}, \\
 C_{ts} &= b_{41}e^{b_{42}v_{SOC}} + b_{43}, R_{tl} = b_{51}e^{b_{52}v_{SOC}} + b_{53}, \\
 C_{tl} &= b_{61}e^{b_{62}v_{SOC}} + b_{63}, C_b = 3600 \cdot \text{Capacity},
 \end{aligned} \quad (11)$$

where b_{ij} are empirically-extracted regression coefficients, while Capacity denotes the nominal energy capacity of the battery. Notice that all circuit model component values, such as value of R_s , R_{ts} , etc., are easily calculated from these equations based on v_{SOC} and Capacity data.

We obtain the discharging characteristics of Li-ion battery by measuring and extracting the regression coefficients for (11). Table 4 shows the parameters for the GP1051L35 Li-ion cell 2-cell series battery pack of 350 mAh capacity with the measurement result of various pulsed discharging and constant discharging currents.

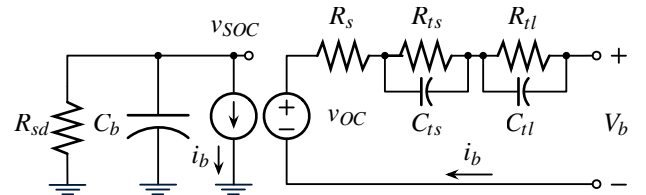


Figure 10: Li-ion battery equivalent circuit model.

Table 4: Extracted parameters for the battery model.

b_{11}	-0.669	b_{12}	-16.208	b_{13}	-0.035
b_{14}	1.280	b_{15}	-0.399	b_{16}	7.553
b_{21}	0.104	b_{22}	-4.325	b_{23}	0.344
b_{31}	0.151	b_{32}	-19.602	b_{33}	0.188
b_{41}	-72.389	b_{42}	-40.832	b_{43}	102.803
b_{51}	2.071	b_{52}	-190.412	b_{53}	0.203
b_{61}	-695.302	b_{62}	-110.630	b_{63}	611.504

5.3 Battery setup optimization

We can change the distribution of the battery output (system input) voltage, V_{bat} by changing the connection of the battery cells. V_{bat} is determined by the number of battery cells in series. Li-ion battery typically has 3.7 V output voltage per cell. If we connect two cells in series, then V_{bat} would be 7.4 V. If we connect three cells in series, then V_{bat} would be 11.1 V. Figure 11 shows the distribution of V_{bat} during 1/2C discharging for GP105L35 Li-ion cell [1]. We use a Li-ion cell which has small capacity during characterization to shorten the experiment time. We measure the voltage and use its distribution to calculate the system efficiency.

We estimate the average power consumption of the system, $\overline{P_{sys}}$, by summing the expectation of each power component power consumption, which is given by

$$\overline{P_{sys}} = \sum_{i=1}^n \int_{I_{min}}^{I_{max}} V_{supply}^i Pr(I_{out}^i = I) IdI, \quad (12)$$

where I_{min} and I_{max} denote the minimum and maximum value of i -th component current I_{out}^i . $Pr(I_{out}^i = I)$ represents the probability that I_{out}^i equals to I . V_{supply}^i is the supply voltage for i -th component. I_{min} , I_{max} , and I_{out}^i are obtained from the measurement result in Section 4.3. We estimate the expectation of system level power loss, $\overline{P_{loss}}$, in similar way. Each $P_{loss}^{conv,i}$ is integrated and then summed with the probability of each loss current, which is given by

$$\overline{P_{loss}^{sys}} = \sum_{i=1}^n \int_{I_{min}}^{I_{max}} P_{loss}^{conv,i}(V_{in}, V_{out}, I) Pr(I_{out}^i = I) IdI, \quad (13)$$

where $P_{loss}^{conv,i}$ is calculated by (9) and (10) with the coefficient in Table 6.

We calculate the internal loss of battery with the internal loss R_s , R_{ts} , and R_{tl} . We ignore the transient aspect of battery loss to

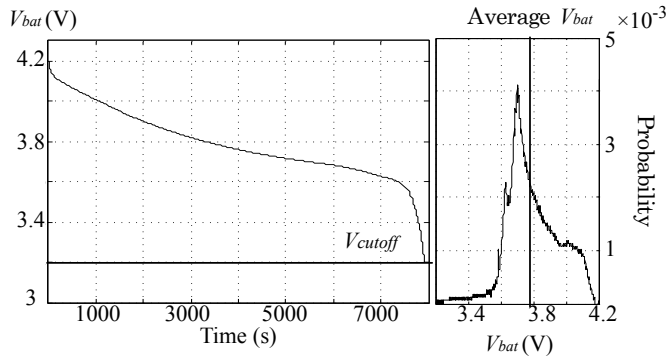


Figure 11: V_{bat} curve and distribution during discharging with average power.

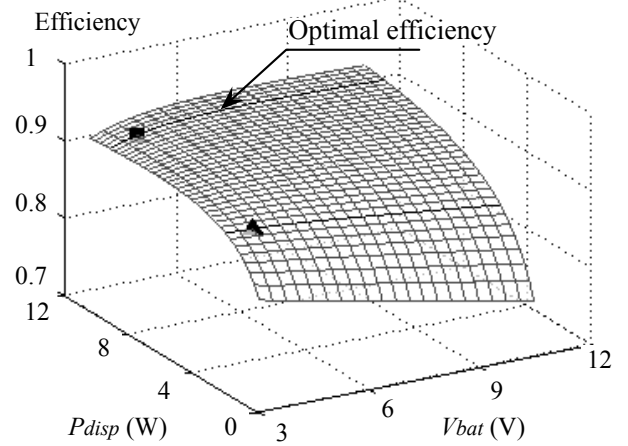
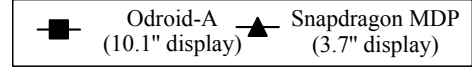


Figure 12: Simulation result of $\eta_{overall}$ for different V_{bat} and P_{disp} without OLED DVS.

simplify the model because the simulation time is order of hour.

$$\begin{aligned} P_{batt} &= P_{sys} + P_{loss}^{sys} + P_{loss}^{batt} = I_{batt} V_{batt}, \\ P_{loss}^{batt} &= I_{batt}^2 (R_s + R_{ts} + R_{tl}), \\ \overline{P_{loss}^{batt}} &= \int_{I_{min}}^{I_{max}} P_{loss}^{batt}(V_{batt}, I) Pr(I_{batt} = I) IdI, \end{aligned} \quad (14)$$

We use the measured R_s , R_{ts} , and R_{tl} values presented in Table 8.

The output power from battery is equals to the sum of power consumption and power loss: Finally, we get the overall efficiency, $\overline{\eta_{overall}}$, by

$$\overline{\eta_{overall}} = \frac{\overline{P_{sys}}}{\overline{P_{batt}}}. \quad (15)$$

Figure 12 shows the aspect of system-level efficiency with different display power consumption, P_{disp} , and battery output (system input) voltage, V_{bat} . We use the OLED cell model introduced in [4] and TFT model introduced in [22] to estimate the average power consumption of different sized OLED panel. Solid lines with the markers in Figure 12 respectively indicate the estimated power efficiency of 220x176 and 1024x768 resolution displays which correspond to 3.7" and 10.1" size, respectively. As shown in Figure 12, we can maximize the efficiency of 2.2" and 10.1" size displays with 1-cell and 2-cell Li-ion battery respectively. If we use 1-cell battery, overall efficiency will decrease when the P_{disp} is larger than about 5 W.

The OLED DVS reduce the effect of voltage difference on the conversion efficiency because it reduce the supply voltage for display on average. Figures 13 shows $\eta_{overall}$ with OLED DVS-enabled system. The overall power consumption of the display is reduced, which results in the optimal number of battery cells in series in generally decreased. The optimal V_{batt} moves toward 1-cell battery compared to the case without DVS.

6. CONCLUSION

OLED display-equipped modern mobile devices such as smartphones and table PCs are suffer from rapidly increasing power consumption. Furthermore, traditional power conversion architecture in the mobile computing system is designed only considering the

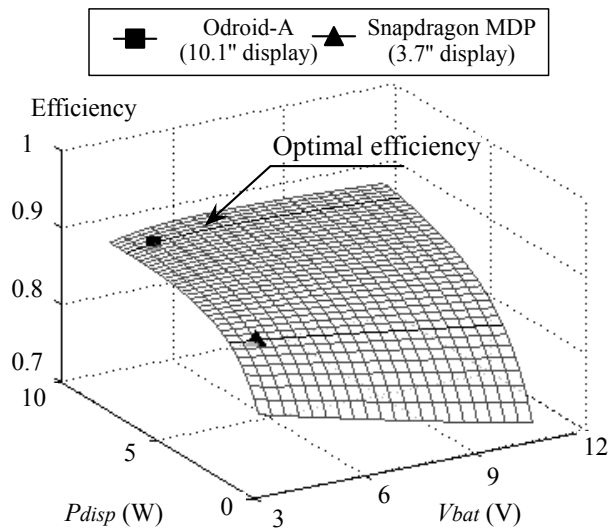


Figure 13: Simulation result of $\eta_{overall}$ for different V_{bat} and P_{disp} with OLED DVS.

fixed supply voltage condition where the system-level low-power techniques such as DVFS are mandatory.

The OLED DVS is a recently introduced OLED power saving method that enables only minimal pixel distortion, small enough to work with natural images. The idea is to scale down the supply voltage and, in turn, dramatically reduce the wasted power caused by the voltage drop across the driver transistor as well as internal parasitic resistance. The supply voltage for the display devices are generally boosted from the battery input due to the electro-optical characteristics of the display devices. Because the display devices are the major power consumer and the display device is generally the only device which requires boosted supply voltage, the boost conversion condition significantly affect the system-level power efficiency where it is determined by voltage difference among the battery output, the boosted voltage for the display, and the other supply voltage with step-down conversion. Therefore, we need to consider the effect on the system-level power efficiency when we integrate the power condition changing low-power techniques such as the OLED DVS.

In this paper, we characterize the power conversion architecture and efficiency of modern smartphone development platform and analyze the effect of the display power condition on the whole system power efficiency. Then we perform the system-level optimization of power conversion architecture with the battery setup by a systematic method instead of the legacy design rule. The estimation result shows that we can expect higher power conversion efficiency with 2-cell Li-ion batteries when the size and power consumption of the displays are growing (which means that portion of the boosted power is growing). The battery setup and charging circuit have been standardized for several decades. It is clear that the legacy design rule cannot guarantee the optimal solution anymore, but it requires significant effort to change the standard. The OLED DVS may slacken this tendency by reducing the boosting voltage on average. The one who designs the mobile systems should understand the characteristics of the components and the mechanism of power conversion to find appropriate solution which cannot be found by just following the legacy design rule without systematic analysis.

7. REFERENCES

- [1] W. Lee and et al., "Power conversion efficiency characterization and optimization for smartphones," in *ISLPED*, 2012.
- [2] Qualcomm, "Snapdragon MDP MSM8660 datasheet," <https://developer.qualcomm.com/develop/development-devices>.
- [3] Samsung mobile display, *AMS369FG01 AMOLED display panel datasheet*.
- [4] D. Shin and et al., "Dynamic voltage scaling of OLED displays," *DAC*, 2011.
- [5] W. Yuan and et al., "Energy-efficient soft real-time cpu scheduling for mobile multimedia systems," *SOSP*, 2003.
- [6] A. Shye and et al., "Into the wild: Studying real user activity patterns to guide power optimizations for mobile architectures," *MICRO*, 2009.
- [7] L. Zhang and et al., "Accurate online power estimation and automatic battery behavior based power model generation for smartphones," *CODES/ISSS*, 2010.
- [8] A. Pathak and et al., "Fine-grained power modeling for smartphones using system call tracing," *EuroSys*, 2011.
- [9] Y. Kim and et al., "System-level online power estimation using an on-chip bus performance monitoring unit," *IEEE Trans. on Computer-Aided Design of Integrated Circuits and Systems*, vol. 30, pp. 1585–1598, November 2011.
- [10] S. Gurun and et al., "A run-time, feedback-based energy estimation model for embedded devices," in *CODES+ISSS*, pp. 28–33, 2006.
- [11] M. Dong and et al., "Self-constructive high-rate system energy modeling for battery-powered mobile systems," *MobiSys*, 2011.
- [12] Y. Choi, , and et al., "DC-DC converter-aware power management for low-power embedded systems," *IEEE Trans. on Computer-Aided Design of Integrated Circuits and Systems*, 2007.
- [13] P. Rong and et al., "An analytical model for predicting the remaining battery capacity of Lithium-ion batteries," *IEEE Trans. on Very Large Scale Integration Systems*, 2006.
- [14] D. Rakhmatov, "Battery voltage modeling for portable systems," *ACM Trans. on Design Automation of Electronic Systems*, 2009.
- [15] L. Benini and et al., "Discrete-time battery models for system-level low-power design," *IEEE Trans. on Very Large Scale Integration Systems*, 2001.
- [16] M. Chen and et al., "Accurate electrical battery model capable of predicting runtime and I-V performance," *IEEE Trans. on Energy Conversion*, 2006.
- [17] J. Jacobs and et al., "Drivers for OLEDs," in *IEEE Industry Applications Conference*, pp. 1147–1152, 2007.
- [18] M. I. Product, *MAX1790/MAX8715 low-noise setp-up DC-DC converter datasheet*, 2005.
- [19] Sumida, *CDMC6D28NP SMD power inductor datasheet*, 2011.
- [20] Diode Incorporated, *B120/B 1.0A surface mount Schottky barrier rectifier datasheet*, 2010.
- [21] Taiyo yuden, *Electrolytic capacitor specifications*. <http://www.yuden.co.jp/>.
- [22] Min-Hao and et al., "Power consumption and temperature increase in large area active-matrix OLED displays," *Journal of Display Technology*, vol. 4, pp. 47–53, march 2008.